Transactions, SMiRT-25
Charlotte, NC, USA, August 4-9, 2019
Division VII

SEISMIC SOIL-STRUCTURE INTERACTION ANALYSIS OF AN EMBEDDED STRUCTURE WITH PARTIALLY BONDED SIDE-SOIL

Cameron B. Samuelson-Sanford[1], Juan M. Jimenez-Chong[2], Mohamed M. Talaat[3], Philip S. Hashimoto[4], David K. Nakaki[5], Oleg Maslenikov[6], James J. Johnson[7]

[1] Senior Staff II, Simpson Gumpertz & Heger Inc., Newport Beach, CA, USA (cbsanford@sgh.com)
[2] Staff II, Simpson Gumpertz & Heger Inc., Newport Beach, CA, USA (jmjimenez-chong@sgh.com)
[3] Senior Project Manager, Simpson Gumpertz & Heger Inc., Newport Beach, CA, USA
Adj. Asst. Prof., Dept. of Structural Engineering, Cairo University, Egypt (mtalaat@sgh.com)
[4] Senior Principal, Simpson Gumpertz & Heger Inc., Newport Beach, CA, USA (pshashimoto@sgh.com)
[5] Senior Project Manager, Simpson Gumpertz & Heger Inc., Newport Beach, CA, USA
(dknakaki@sgh.com)
[6] Senior Consultant, James J. Johnson and Associates, Alamo, CA, USA (omaslenikov@gmail.com)
[7] President, James J. Johnson and Associates, Alamo, CA, USA (jasjjoh@aol.com)

ABSTRACT

Seismic soil-structure interaction (SSI) analysis is performed for an embedded structure with partially bonded side-soil in support of the seismic probabilistic risk assessment of a nuclear power plant. Adjacent buildings with shallower embedment shield the subject structure on all four sides from soil over their embedded depths, creating a partially bonded condition where soil is not in full contact with the sides of the structure up to grade. An efficient, state-of-the-art, hybrid method employing computer programs SASSI2010 [Ostadan and Deng, (2010)], RIGID2017, and CLASSI [Luco and Wong (1980)], as presented in Johnson et al. (2019), is used for this analysis.

The hybrid method takes advantage of the capability of SASSI2010 and RIGID2017 to analyze embedded structures with partially bonded side-soil and the computational efficiency of CLASSI to rapidly perform the SSI response analysis of large structure models. RIGID2017 imposes rigid constraints in the embedded region to allow for the determination of impedance and scattering functions.

Impedance functions, scattering functions, and in-structure response spectra (ISRS) are compared between analyses that consider various side-soil bonding heights. These comparisons show the effects of partial embedment and substantiate the results.

CONTEXTUAL REVIEW

A Reactor Building (RB) is surrounded on all four sides by other buildings, which are founded at various depths, such that the RB is shielded from the soil over their embedded depths. Computer program RIGID2017 is modified to generate impedance and scattering matrices for the embedded RB considering partial bonding with the side-soil by modeling loss of support of the side-soil along a partial depth. The unbonded depth can be specified between zero and the full embedment depth. The impedance matrix describes the complex-valued force-displacement relationship between the foundation and surrounding soil at a single reference point with six degrees of freedom. The scattering matrix defines the ratios between the free-field motion input at the control point (the soil surface in this study) and the input motion at the foundation reference point.

This paper investigates the capability of RIGID2017 to evaluate various side-soil bonding heights in support of probabilistic seismic response analyses of the RB, including effects of SSI. Some of the results presented herein are a subset of the full probabilistic analyses, which are performed following the general methodology described in Nakaki et al. (2015) using the hybrid approach presented in Johnson et al. (2010).

The probabilistic response analyses are of two types. The first captures composite variability from both randomness and uncertainty, including ground motion, soil stiffness and damping, structure frequency, and structure damping. The second captures the randomness contribution of the earthquake motion by only varying the input time history and assigning median values to the other parameters. For simplicity, this paper focuses on the results of the randomness-only analysis that uses median structure and soil properties, with only brief mention of some composite variability results.

To support this analysis, capabilities of RIGID2017 are expanded from a previous version to allow for generation of impedances and scattering functions of an embedded foundation considering partial bonding with the side-soil. The previous version was limited to modeling all side-soil as fully bonded. Among other advantages, this allows for more flexibility in modeling the side-soil without introducing simplifications such as removing the top layers of unbonded side-soil from the model altogether.

Deconvolution of the surface motion to the RB foundation is modeled in SASSI2010 and represented by frequency-dependent, complex-valued scattering matrices. Deconvolution of the motion from the surface caused valleys in individual free-field response spectra at the foundation level used in the probabilistic analysis. This was considered acceptable since probabilistic seismic response analysis was performed and the effective soil-column frequency was varied, which shifted the valleys between multiple simulations. The resulting 50% (median) and 84% non-exceedance probability (NEP) input spectra at the foundation level did not exhibit deficiencies characterized by valleys in any frequency band.

This novel hybrid SSI modeling technique coupled with probabilistic seismic response analysis eliminates the need to perform additional site response analyses to develop foundation input response spectra (FIRS) for this structure. FIRS would be required if a more traditional SSI technique is employed where the RB is modeled with only the bonded side-soil depth included in the analysis (e.g., with unbonded side-soil completely removed), or if deterministic seismic response analysis is performed.

PROBLEM STATEMENT

To assess the effects of various side-soil bonding heights, RB impedances are determined by modeling five different conditions. The first two conditions, which serve as baselines to compare other results to, are modeled by (1) fully bonding all side-soil up to the soil surface at Elevation 440 ft and (2) modeling the RB as surface-founded at Elevation 406 ft by removing all side-soil. The other three conditions are modeled using the hybrid approach to model bonded side-soil to heights of 2 ft, 10 ft, and 23 ft above the bottom of the RB foundation. These heights correspond to Elevations 408 ft, 416 ft, and 429 ft, respectively. The conditions with 2 ft and 10 ft bonded heights are expected to have similar impedance function trends to the baseline case with the side-soil removed, while the condition with a 23 ft bonded height is expected to have similar trends to the baseline case with fully bonded side-soil. The free-field input control motion is defined at the soil surface.

STRUCTURE MODEL

The RB is a concrete shear wall structure with plan dimensions of 135 ft by 151 ft in the north-south and east-west directions, respectively. It is founded on a reinforced concrete basemat that is 16 ft thick with plan dimensions of 147 ft by 157 ft. A steel superstructure rises about 60 ft above the refueling floor.

A fixed-base finite element model representing median properties of the RB (Figure 1) is developed following the guidance of ASCE/SEI 4-16 [American Society of Civil Engineers (2017)]. The model represents the significant seismic load-resisting structural components. The X (or 1) axis is oriented toward the east, the Y (or 2) axis is oriented toward the north, and the Z (or 3) axis is oriented upward. The basemat is not included in the fixed-base model because it is included in the subsequent SSI analyses. A fixed-base modal analysis is performed using the Ritz vector method. Modal damping values are calculated for the SSI analysis using a stiffness-weighted approach consistent with the composite modal damping approach described in ASCE/SEI 4-16. Frequencies, damping values, and fractions of total mass participation for selected fixed-base modes are listed in Table 1.

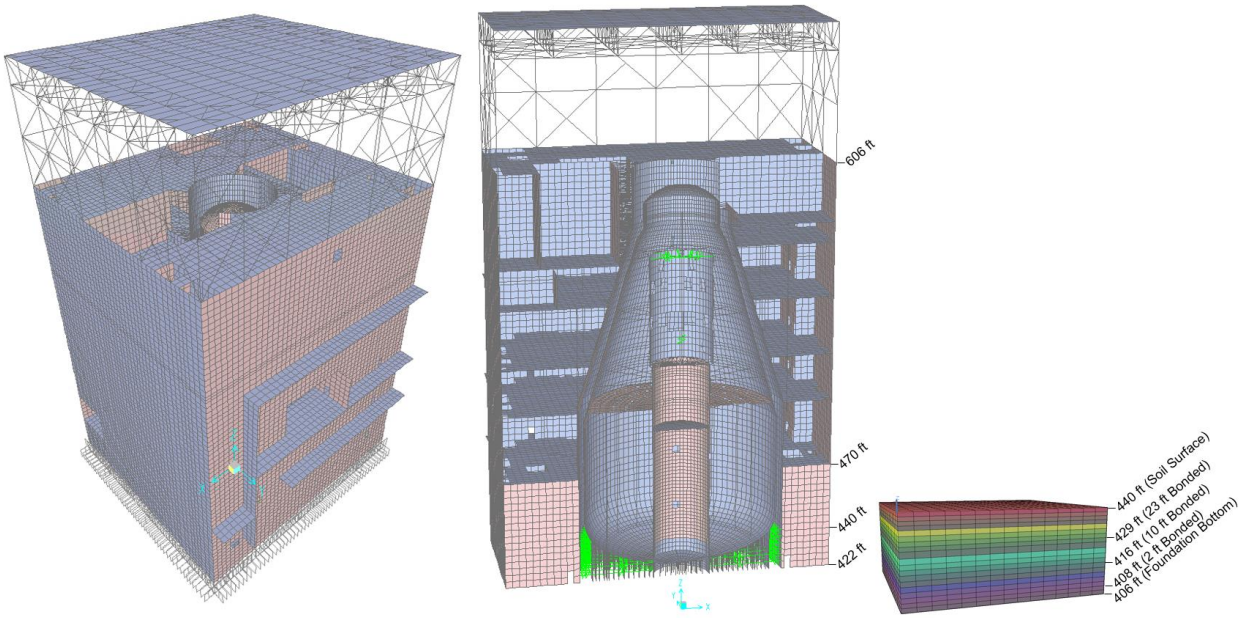

(a) Exterior View Looking Southwest (b) Interior View Looking North (c) Excavated Soil Model
Figure 1. Structure Model & Median Excavated Soil Model

Table 1: Fixed-Base Structure Model Modes and Damping

Mode	Frequency	Damping	Percent of Total Mass Participation			Description
	Hz		X	Y	Z	
2	2.78	6.61%	0.1%	66.0%	0.0%	Overall Y-direction Mode
3	2.93	6.55%	65.3%	0.1%	0.0%	Overall X-direction Mode
106	9.18	4.18%	2.3%	0.0%	10.5%	Overall Vertical Modes
107	9.20	4.01%	1.9%	0.0%	7.2%	
124	9.89	5.25%	2.6%	0.0%	10.8%	
126	9.95	5.74%	2.4%	0.0%	10.5%	
154	10.81	5.22%	0.0%	0.0%	5.3%	

SOIL-STRUCTURE INTERACTION MODELS & ANALYSIS METHODOLOGY

In the hybrid approach, the foundation impedances are calculated using computer programs SASSI2010 and RIGID2017, and the seismic response analysis is performed using computer program CLASSI. The embedded region of the RB is approximated as being rigid since the RB is stiff relative to the soil in which it is embedded.

The first step in the hybrid approach is to perform analyses with SASSI2010 to generate the frequency-dependent, unconstrained, and flexible impedance matrices defining the complex-valued force-displacement relationships between degrees of freedom at the soil-foundation interaction nodes. The second step is to use RIGID2017 to apply the constraints of rigid body motion to the unconstrained/flexible impedance matrix and implement the assumed pattern of spatial variation of the free-field ground motion. This yields the impedance and scattering matrices about a reference point on the foundation.

The third step is to combine results from the first step, second step, and fixed-base structural model to solve the complete SSI problem. This involves calculating the SSI response of the foundation including the effects of the structure (fixed-base modes), foundation (mass), and supporting soil (impedance functions) when subjected to the foundation input motion. Then the foundation SSI response is used to calculate dynamic responses of structure degrees-of-freedom.

As part of the analysis described above, excavated soil layers displaced by the embedded foundation are discretized vertically in order to transmit adequate frequency content in the input motion through the soil. Finite element models of the excavated soil replaced by the embedded structure are developed (Figure 1c) and the SASSI2010 direct method for modeling the excavated soil is used. Soil properties are shown in Figure 2. The ground motion input is defined at the soil surface.

The 50% and 84% NEP ISRS are calculated at select RB locations following the approach summarized in Nakaki et al. (2015). For simplicity, this paper only examines median ISRS of the randomness-only analysis that uses median structure and soil properties.

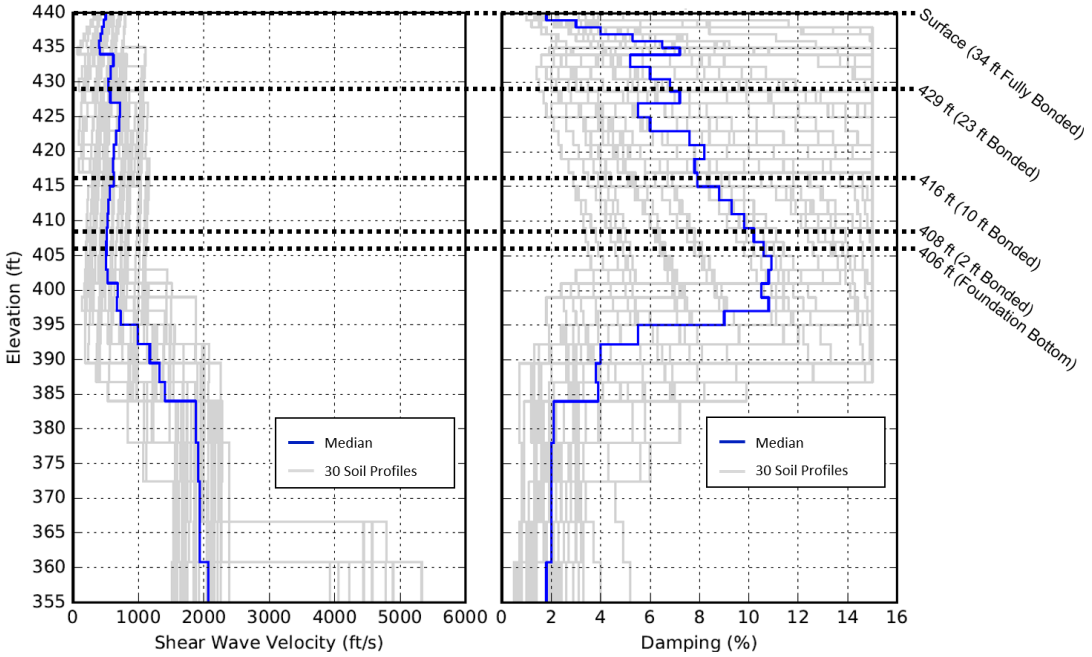

Figure 2. Soil Properties

ANALYSIS RESULTS

Impedance and scattering values plotted herein are normalized to a foundation characteristic length (R) of 86 ft and the shear modulus (G) of the soil layer property immediately under the foundation. Since the foundation is nearly square in plan, impedance term K22 (Y-direction translation impedance value) is similar to term K11 (X-direction translation impedance value), term K44 (XX-rocking impedance value) is similar to term K55 (YY-rocking impedance value), and term K24 (coupled Y-direction and XX-rocking impedance value) is similar to term K15 (coupled X-direction and YY-rocking impedance value) but of opposite sign. Analogously, scattering terms S22 and S11 are similar, and S42 and S51 are similar but of opposite signs.

Figure 3 plots median soil profile impedance values for the five different side-soil bonding conditions: no side-soil (i.e., surface-founded at Elevation 406 ft without embedment) and bonded side-soil to heights of 2 ft, 10 ft, 23 ft, and 34 ft (i.e. all side-soil is fully bonded). Impedance functions for the median soil profile with various side-soil bonding heights are generally similar below about 15 Hz, with more significant differences above 15 Hz. Static impedance values show an increase in magnitude with side-soil bonding height due to the increased stiffness provided by increased side-soil bonding. Despite this trend in static values, impedance function shapes for all cases are somewhat similar between 3 Hz and 15 Hz with no qualitative contrast due to side-soil bonding height. However, real impedance values above about 15 Hz generally increase in magnitude with increased side-soil bonding. This trend is unique to the site soil and is not as straightforward as it would be for a simplified configuration with uniform soil properties.

Figure 4 plots median soil profile scattering values for bonded side-soil to heights of 2 ft, 10 ft, 23 ft, and 34 ft (i.e. fully bonded). All scattering functions (S11, S51, and S33) are comparable for cases with 2 ft and 10 ft bonded heights, while a 23 ft bonded height produces similar scattering value trends to the baseline case with fully bonded side-soil. As anticipated, this shows that the cases with the least bonding have divergent results from the cases with the most bonding. S11 scattering values increase in magnitude as the side-soil bonding height decreases. This trend occurs because the rigid embedment transfers horizontal motion through the height of the bonded side-soil, such that the motion at the base of the foundation is more similar to the surface motion for the case with fully bonded side-soil than for the cases with smaller bonding heights. In other words, the side-soil is less constrained with smaller bonded heights, which leads to higher peaks in the S11 plots. S33 scattering functions have valleys near 12 Hz, 14 Hz, 21 Hz, and 22 Hz for the 2 ft, 10 ft, 23 ft, and fully bonded cases, respectively. These valleys are partially influenced by the soil-column frequencies of the side-soil. The S51 scattering functions for fully bonded side-soil show higher magnitudes around 25 Hz than for a bonding height of 2 ft because, as anticipated, the fully bonded condition has more influence on rocking of the embedded structure due to horizontal motion at the surface.

Normalized K11 impedance functions for the softest and stiffest soil profiles of thirty used in the probabilistic analyses are compared in Figure 5. Three side-soil bonding conditions are plotted: surface founded with no side-soil, 23 ft of bonded side-soil, and fully bonded side-soil up to the soil surface. The embedded values match the surface-founded results very closely at low frequencies, below about 7 Hz, for the softest soil profile because the side-soil is relatively soft and contributes minimally to embedment effects. Conversely, more deviation between the embedded results and surface founded results at low frequencies is evident for the stiffer soil profile. The embedded values start to considerably deviate from the surface-founded results at about 10 Hz for the softest soil profile, about 20 Hz for the median soil profile (Figure 3), and above 25 Hz for the stiffest soil profile. These likely correspond to the soil system frequencies, i.e., those that result from the soil-column and constraints provided by bonded side-soil without the influence of the structure and foundation mass. For each individual case, this indicates that more of the side-soil stiffness is being engaged at this frequency.

Figure 6 shows 5% damped median response spectra that consider randomness-only variability at the soil surface and at the center of the foundation. The first peak of the Y-direction and XX-rotation spectra for each case corresponds to the SSI system frequency, while the second peak is associated with the peak of the free-field input motion. As the side-soil bonding height increases, the SSI system frequency gradually increases from about 1.4 Hz for 2 ft of bonded side-soil to about 1.7 Hz for fully bonded side-soil. This is a result of increased stiffness provided by increased side-soil bonding, i.e., higher impedance. The SSI system filters the input motion and shifts energy content away from the input motion peak to the SSI frequency, such that the second peak generally decreases and the valley between the two peaks gets wider as the SSI frequency decreases and shifts away from the input motion peak. Accordingly, the second peak is reduced with decreased side-soil bond height, except for the 2 ft bond height case which has a larger peak than the rest. This larger peak is likely due to resonance of the side-soil column frequency (about 4 Hz) with the peak of the free-field input motion. Nevertheless, the second peak of the Y-direction foundation spectra are less than the peak of the free-field spectra for all side-soil bonding heights.

Figure 7 shows 5% damped median ISRS that consider randomness only variability at the corner of the floor at Elevation 470 ft, located just above the soil surface, and at the top corner of the concrete structure (Elevation 606 ft). Comparison of Figures 6 and 7 shows that magnitudes of the first spectral peak increase but magnitudes of the second peak stay about the same with increased height in the RB. This emphasizes the fundamental SSI frequencies shown by the foundation spectra and the fact that the second peak corresponds to the peak of the free-field input motion. SSI frequencies are significantly less than the fixed-base frequency of 2.78 Hz. This difference signifies that the fundamental horizontal modes of the soil-structure system are dominated by translation and rocking of the relatively stiff structure on flexible soil.

The horizontal ISRS at Elevation 606 ft (Figure 7) shows that the zero-period acceleration (ZPA) increases with increased side-soil bond height. This is expected because the shape of the input spectrum leads to increased spectral acceleration demand with increased frequency due to increased bond height. As the height in the structure decreases, the difference between ZPAs of the different side-soil bond cases typically decreases, as expected. For the case with 2 ft of bonded side-soil, as the height in the structure decreases, the horizontal ZPA gradually surpasses ZPAs for other bond heights, such that this case has the highest ZPA at the foundation (Figure 6 and 7). This confirms that the increase in ZPA at the foundation for the 2 ft bonded case is a local foundation response caused by alignment of side-soil column frequency with the peak of the free-field input motion.

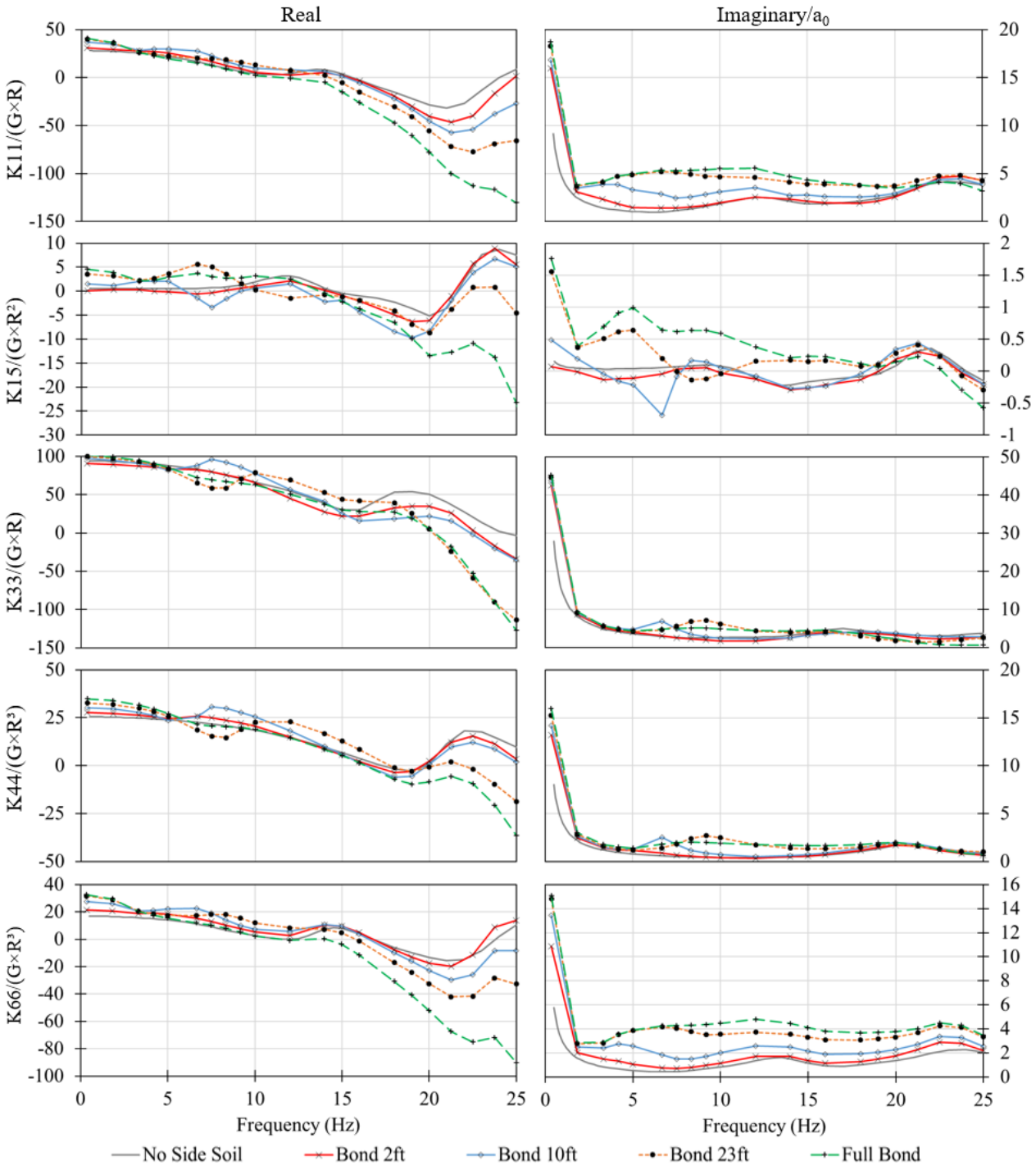

Where: G = 843 kip / ft ^{2}, R = 86 ft, and a_o = freq. / 0.943

Figure 3**.** Normalized Impedance Functions

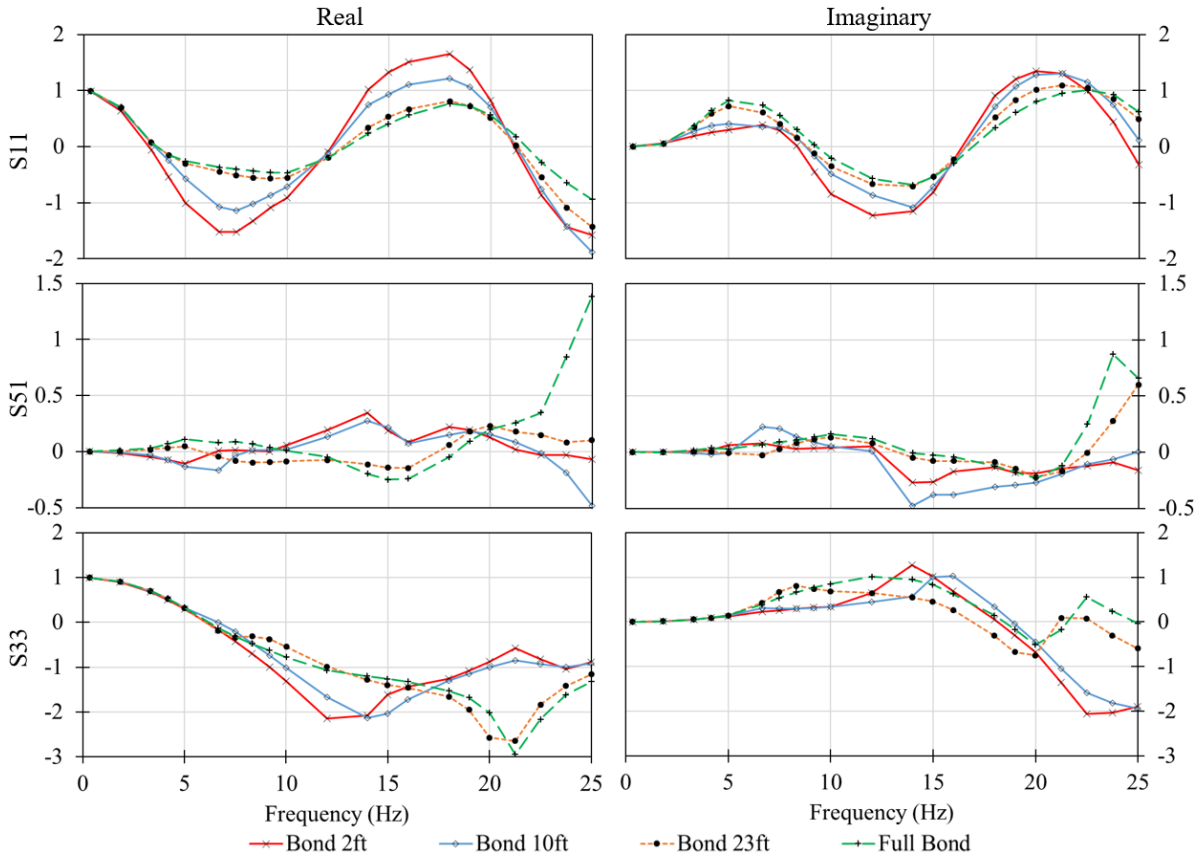

Figure 4. Scattering Functions

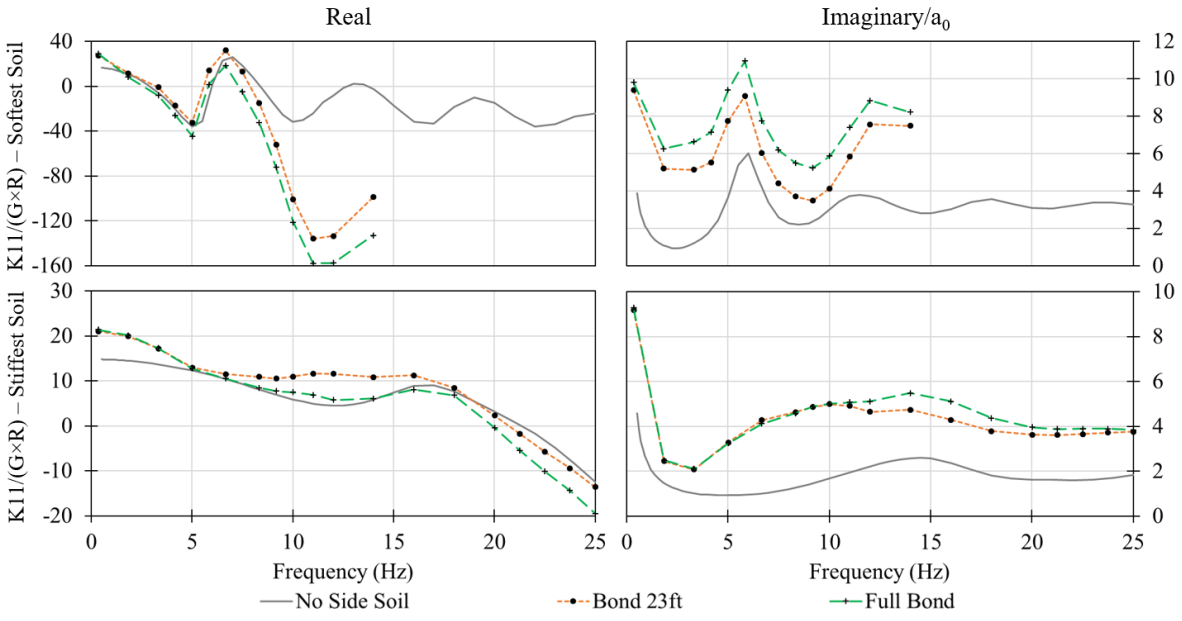

Where: G = 142 kip / ft ^{2}, R = 86 ft, and a_o = freq. / 0.388 for the Softest Soil
G = 4,090 kip / ft ^{2}, R = 86 ft, and a_o = freq. / 2.08 for the Stiffest Soil

Figure 5. Soft and Stiff Soil Profile Normalized Impedance Comparison

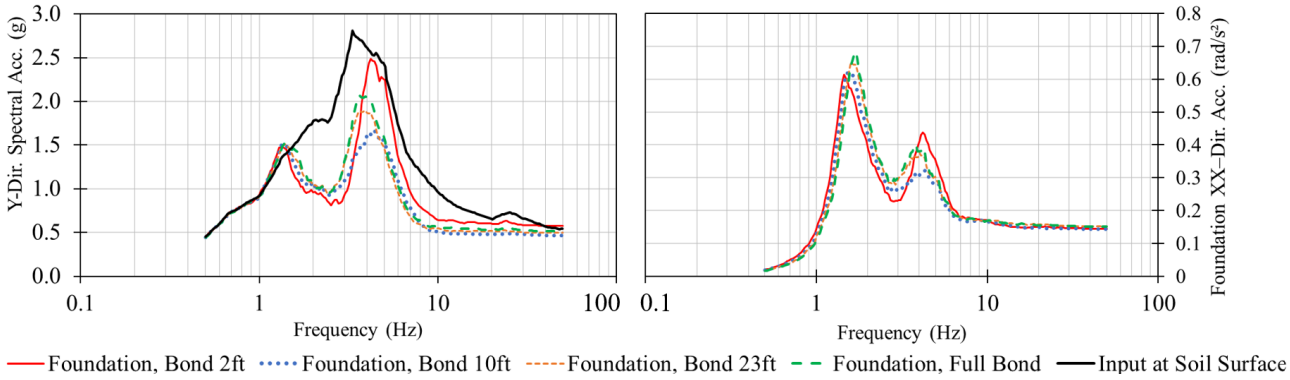

Figure 6. Median Input and Foundation Response Spectra

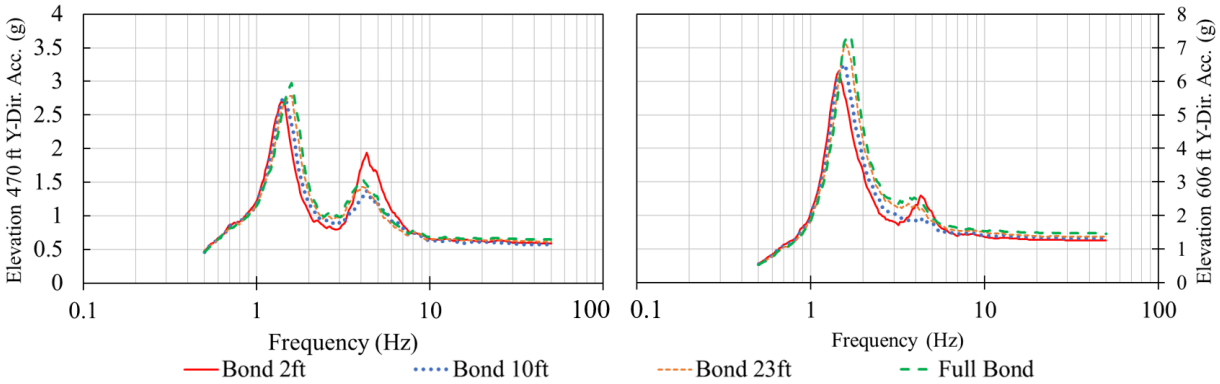

Figure 7. Median In-Structure Response Spectra at the Southwest Corner of the Structure

SUMMARY & CONCLUDING REMARKS

Impedance and scattering function plots for an embedded structure, generated using computer programs SASSI2010 and RIGID2017, for three different side-soil bonding heights are compared to each other and to two baseline cases modeled by (1) fully bonding all side-soil up to the soil surface and (2) modeling the RB as surface-founded by removing all side-soil. The hybrid method for partially bonded embedded structures, presented in Johnson et al. (2019) is used to perform seismic response analyses of the structure, including effects of SSI. Impedances and ISRS are compared between the multiple side-soil conditions. Several observations from these comparisons are summarized below, which show some effects of partial embedment and substantiate the results of this unique soil-structure model:

- Impedance values generally increase in magnitude with side-soil bonding height due to the increased stiffness provided by increased side-soil bonding.
- Horizontal scattering values decrease in magnitude as the side-soil bonding height increases because the rigid embedment constrains horizontal motion through the height of the bonded side-soil.
- Impedance values for the embedded structure are close to the surface-founded results at static and low-frequency conditions for a soft soil profile because the side-soil contributes minimally to embedment effects. Conversely, more contrast between the embedded and the surface-founded impedances at low frequencies is evident for a stiffer soil profile.
- The SSI system frequency increases as a result of increased stiffness provided by increased side-soil bonding.

- The SSI system filters the input motion and shifts energy content away from the input motion peak to the SSI frequency such that, with decreased side-soil bond height, foundation spectra show decreased amplitude at the input motion peak and a wider, deeper valley between the SSI frequency peak and the input motion peak.
- ZPAs increase with increased side-soil bond height because the shape of the input spectrum leads to increased spectral acceleration demand with increased frequency.

ACKNOWLEDGEMENT

The authors gratefully acknowledge Dr. Robert P. Kennedy's encouragement and support in the development of this approach for modeling partially bonded embedded foundations and its implementation in an actual evaluation.

REFERENCES

American Society of Civil Engineers (2017), *Seismic Analysis of Safety-Related Nuclear Structures and Commentary*, *ASCE/SEI 4-16*, Reston, VA.

Johnson, J.J., Maslenikov O.R., Nakaki D.K., Talaat M.M., Jimenez-Chong J.M., and Samuelson-Sanford C.B. (2019), "A Hybrid SSI Analysis Method for Embedded and Partially Bonded Foundations," *SMiRT-25*, Charlotte, NC.

Johnson, J.J., Maslenikov O.R., Nakaki D.K., Hashimoto P.S., Bayraktarli Y.Y., and Zuchuat O. (2010), "A Hybrid Method to Develop SSI Parameters for Rigid Embedded Foundations of Arbitrary Shape," *Proceedings of the ASME 2010 Pressure Vessel and Piping Division Conference*, American Society of Mechanical Engineers, New York, New York.

Luco, J.E. and Wong H.L. (1980), *Soil-Structure Interaction: A Linear Continuum Mechanics Approach (CLASSI)*, *Report No. CE79-03*, University of Southern California, Los Angeles, CA.

Nakaki, D.K., Hashimoto P.S., Samuelson-Sanford C.B., Ryan M.J., and Bayraktarli Y.Y. (2015), "Seismic Response Analysis of the Mühleberg Nuclear Power Plant Structures for the PEGASOS Refinement Project," *SMiRT-23*, Manchester, United Kingdom.

Ostadan, F. and Deng N., (2010), *SASSI2010, A System for Analysis of Soil-Structure Interaction, Theoretical Manual*, University of California, Berkeley, Version 1.